

Fluorescence enhancement and nonreciprocal transmission of light waves by nanomaterial interfaces

M. Nyman,^{*} A. Shevchenko,[†] and M. Kaivola*Department of Applied Physics, Aalto University, P.O. Box 13500, FI-00076, Aalto, Finland*

(Received 12 September 2017; published 13 November 2017)

In an optically absorbing or amplifying linear medium, the energy flow density of interfering optical waves is in general periodically modulated in space. This makes the wave transmission through a material boundary, as described by the Fresnel transmission coefficients, nonreciprocal and apparently violating the energy conservation law. The modulation has been previously described in connection to ordinary homogeneous nonmagnetic materials. In this work, we extend the description to nanomaterials with designed structural units that can be magnetic at optical frequencies. We find that in such a “metamaterial” the modulation in energy flow can be used to enhance optical far-field emission in spite of the fact that the material is highly absorbing. We also demonstrate a nanomaterial design that absorbs light, but simultaneously eliminates the power flow modulation and returns the reciprocity, which is impossible to achieve with a nonmagnetic material. We anticipate that these unusual optical effects can be used to increase the efficiency of nanostructured light emitters and absorbers, such as light-emitting diodes and solar cells.

DOI: [10.1103/PhysRevA.96.053828](https://doi.org/10.1103/PhysRevA.96.053828)

I. INTRODUCTION

The details of the flow of light energy inside an absorbing material are usually not an object of close attention, because only outside the medium is this energy typically of relevance. A notable exception is fluorescence, but even in this context absorbing materials are often avoided because they can lead to fluorescence quenching [1]. On the other hand, many materials designed for fluorescence enhancement are absorbing. They include nanostructured plasmonic materials, such as hyperbolic metamaterials which have proved to provide remarkable fluorescence enhancement [2–6]. However, in such media, light produced by the enhanced fluorescence is usually considerably attenuated by absorption and surface reflection before it escapes from the material.

Optical waves propagating in an absorbing medium can reflect off the boundary with another medium and interfere with themselves. The incident and reflected waves then form a standing wave pattern that in general exhibits spatially modulated absorption. The magnitude of the Poynting vector is modulated as well, and the power flows of the incident and reflected waves become inseparable from each other, which makes the *plane-wave transmission* through the interface nonreciprocal, invalidating the ordinary definition of the power transmission and reflection coefficients in terms of the Fresnel coefficients. Note that the Lorentz reciprocity theorem that does not separate the interfering waves is still satisfied in absorbing media [7]. Due to the same interference effect, the fluorescence or scattering by a particle near the interface can substantially differ from that in a transparent medium [8,9]. Furthermore, a tunability of the phase shift upon reflection inside an absorbing medium can be used to improve the efficiency of ultrathin optical coatings and light energy harvesting devices [10–12].

In this work we show that a nanostructured absorbing medium can be *designed* to enhance optical emission near the material’s boundary by controlling the interference-induced spatial modulation of absorption. We begin by generalizing the absorbing media to include optical metamaterials. In these nanomaterials, the magnetic permeability can differ from the vacuum permeability, unlike in most other materials at optical frequencies [13,14], and the effect of spatial dispersion can be strong [15–18]. Such materials allow one to tune the refractive index and the wave impedance separately [15,16], providing more possibilities for useful applications. Also, we show that, compared to a homogeneous absorbing medium, a metamaterial can be designed to *minimize fluorescence quenching* by placing the emitters in the lossless parts of the material’s structural units [5]. In particular, for optical waves radiated in an absorbing medium toward the material boundary, the medium can appear effectively *fully transparent*. Furthermore, the radiation can even be *enhanced*, which is a counterintuitive result considering the fact that the emitter is inside an absorbing medium. It is remarkable that the origin of the discovered enhancement is fundamentally different from that observed in hyperbolic metamaterials [2]. Finally, we demonstrate an unusual metamaterial that, despite being absorbing, introduces no modulation of optical absorption in the wave interference pattern, which makes the power flows of the waves fully separable again. This property is impossible to achieve with nonmagnetic absorbing materials.

We divide the article into sections as follows: Section II introduces the theoretical tools for analyzing power flows and optical emission in materials, as well as describes our key ideas for practical applications. In Sec. III we present examples of two metamaterials exhibiting the emission enhancement and nonreciprocal transmission effects. Finally, Sec. IV concludes our work.

II. THEORY

Consider a plane wave incident upon an interface between two absorbing or amplifying media that, similar to

*markus.nyman@aalto.fi

†andriy.shevchenko@aalto.fi

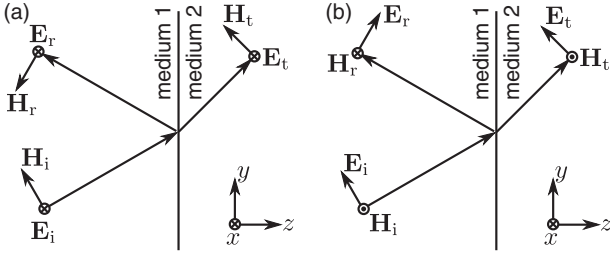


FIG. 1. A plane wave is incident from medium 1 onto an interface between media 1 and 2, and is split into reflected and transmitted waves. TE- and TM-polarized waves are shown in (a) and (b), respectively.

metamaterials, are allowed to be magnetic and spatially dispersive. Figure 1 shows the electric and magnetic fields \mathbf{E}_j and \mathbf{H}_j of the incident ($j = i$), reflected ($j = r$), and transmitted ($j = t$) waves for the TE and TM polarizations. We assume that the wave parameters, such as the refractive index n_i and impedance Z_i are known for all possible directions of propagation in medium 1 ($i = 1$) and medium 2 ($i = 2$). Note that this information is enough to fully characterize optical properties of any anisotropic and spatially dispersive material with higher-order multipole excitations in its structural units [17,18]. In some cases, however, when strong evanescent-wave coupling is present between the metamaterial layers, the wave parameters can yield inaccurate calculation results [15–18].

To make our results independent of polarization, we introduce a *tangential impedance*, defined as [18]

$$\eta_i = Z_i(\cos \theta)^p, \quad (1)$$

where $p = 1$ for transverse-magnetic (TM) polarization and $p = -1$ for transverse-electric (TE) polarization, and $\theta = \arccos(k_z/k)$ is the complex propagation angle with respect to the z axis (see Fig. 1). The *tangential transmission and reflection coefficients* of the interface are defined as $\tau_{12} = E_{t, \text{tr}}/E_{i, \text{tr}}$ and $\rho_{12} = E_{r, \text{tr}}/E_{i, \text{tr}}$, where $E_{j, \text{tr}}$ denotes the tangential component of the field E_j . The coefficients are given by [18]

$$\tau_{12} = \frac{\frac{2}{\eta_1}}{\frac{1}{\eta_1} + \frac{1}{\eta_2}}, \quad (2)$$

$$\rho_{12} = \frac{\frac{1}{\eta_1} - \frac{1}{\eta_2}}{\frac{1}{\eta_1} + \frac{1}{\eta_2}}, \quad (3)$$

independently of the wave polarization.

The energy flow in the incident, reflected, and transmitted waves is described by the time-averaged Poynting vector

$$\mathbf{S} = \frac{1}{2} \text{Re}\{\mathbf{E} \times \mathbf{H}^*\}. \quad (4)$$

In medium 1 both the incident and reflected waves are present and the z component of the Poynting vector can be written as

$$S_{1z} = \frac{|E_i|^2}{2|\eta_1|^2} \left\{ \text{Re}\{\eta_1\} [e^{-2\alpha_1 z} - |\rho_{12}|^2 e^{2\alpha_1 z}] - 2\text{Im}\{\eta_1\} |\rho_{12}| \sin(2\beta_1 z + \phi) \right\}. \quad (5)$$

This equation is in agreement with Eq. (16) of [8], where, however, the material was assumed to be nonmagnetic. Here,

E_i is the electric-field amplitude of the incident wave at $z = 0$; we also denote $\beta_1 = \text{Re}\{k_{1z}\}$, $\alpha_1 = \text{Im}\{k_{1z}\}$, and $\phi = \arg \rho_{12}$. The first term, proportional to $\text{Re}\{\eta_1\}$, contains the Poynting vectors of the incident and reflected waves, and the second term, proportional to $\text{Im}\{\eta_1\}$, is due to the interference of the incident and reflected waves. The power flows of these waves cannot be separated from each other if $\text{Im}\{\eta_1\} \neq 0$, which is the case also for an ordinary absorbing material. In general, $\beta_1 \neq 0$ and the Poynting vector has a spatially oscillating component due to the standing-wave variation of the electric and magnetic fields. For a typical lossy dielectric, semiconductor, or metal at optical frequencies, the absorption is entirely electric, i.e., due to the imaginary part of ϵ . Hence, in the electric-field maxima of the wave interference pattern, absorption will be highest. Conversely, in the electric-field minima the absorption is lowest. The spatially modulated absorption is then observed as a modulation in the Poynting vector. In optical metamaterials, absorption can take place also due to the imaginary part of μ , or one can have, e.g., $\text{Im}\{\epsilon\} > 0$ and $\text{Im}\{\mu\} < 0$, implying electric absorption and magnetic gain. The medium as a whole will still be absorbing as $\text{Im}\{\eta\} > 0$ [19]. The same applies if $\text{Im}\{\mu\} > 0$ and $\text{Im}\{\epsilon\} < 0$ in a metamaterial without optical gain.

The modulation of the Poynting vector by interference has interesting consequences when it comes to the emission of light inside the medium. For example, the interference of the emitted and reflected waves *can reduce absorption* by the material in the region between the emitter and the interface. In fact, the interference term can contribute either positively or negatively to the energy flow across the interface. However, if medium 2 is lossless, the interference contribution is positive, which can be verified by inserting Eq. (3) into Eq. (5) at $z = 0$.

Any electromagnetic source can be modeled as a distribution of electric current [20]. For example, as a source of a plane wave one can use a planar distribution of current, matched in phase with the wave. Any other distributed or localized source, e.g., a point dipole, can then be constructed as a sum of such plane-wave sources [21]. For a plane wave propagating along z toward the material's boundary at $z = 0$, the current density can be written in the form $\mathbf{J} = \mathbf{K}_0 \delta(z + d) e^{-i\omega t}$, where \mathbf{K}_0 is the surface current density and the source is located at $z = -d$. The source will emit two plane waves, one in the positive and one in the negative z direction. Both waves have the electric-field amplitude

$$E_0 = \frac{\eta}{2} K_0, \quad (6)$$

where η is the tangential impedance of the medium [21].

The Poynting vector in medium 2 can also be written as

$$S_2 = \frac{1}{2} \text{Re} \left\{ \frac{1}{\eta_2} \right\} |E_0|^2 |\tau_{12}|^2 e^{-2\alpha_1 d} e^{-2\alpha_2 z}, \quad (7)$$

where $\alpha_2 = \text{Im}\{k_{2z}\}$. Let us assume that medium 2 is glass with a real-valued refractive index n_2 and impedance η_2 . Inserting Eqs. (2) and (6) into Eq. (7), we find

$$S_2 = \frac{1}{2} \frac{1}{\eta_2} \left| \frac{1}{\eta_1} + \frac{1}{\eta_2} \right|^{-2} |K_0|^2 e^{-2ad}. \quad (8)$$

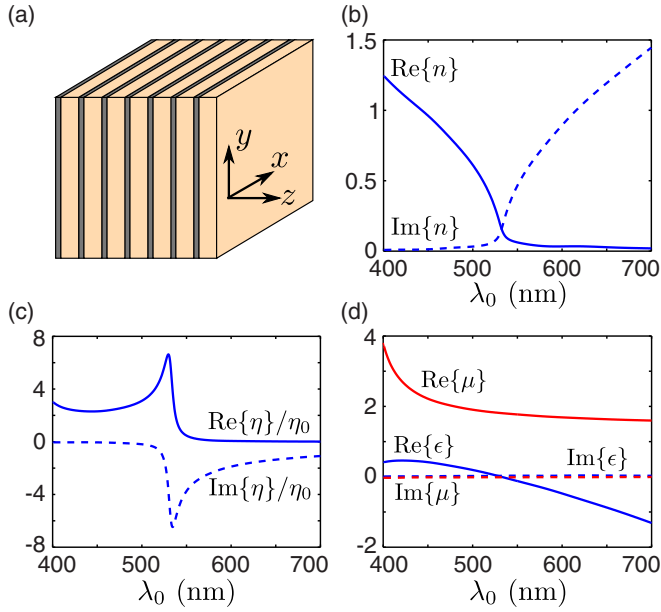


FIG. 2. Metal-dielectric stack metamaterial. (a) Structure. (b) Spectrum of n for normal-incidence waves. (c) Spectrum of η . (d) Spectra of ϵ and μ in blue and red lines, respectively. In all spectra, solid and dashed lines correspond to the real and imaginary parts of the quantities, respectively.

With fixed η_2 , the sum of inverted impedances reaches a minimum value of $1/\eta_2$ when η_1 is very large. To compare the result to the intensity created by the same emitter in glass, we set $\eta_1 = \eta_2$ and obtain $S_2 = |K_0|^2 e^{-2\alpha d} \eta_2/8$. If the impedance of medium 1 is large, we obtain $S_2 = |K_0|^2 e^{-2\alpha d} \eta_2/2$, implying an emission enhancement by a factor of 4. Because the properties of metamaterials can be tuned, the emission enhancement can be harnessed.

While Eq. (5) exhaustively describes the power flow near an interface, it is convenient to introduce also the following power transmission and reflection coefficients:

$$T_{12} = \frac{S_{\text{tr}}}{S_{\text{inc}}} = |\tau_{12}|^2 \frac{\text{Re}\{1/\eta_2^*\}}{\text{Re}\{1/\eta_1^*\}}, \quad (9)$$

$$R_{12} = \frac{S_{\text{ref}}}{S_{\text{inc}}} = |\rho_{12}|^2. \quad (10)$$

Here, S_{tr} , S_{ref} , and S_{inc} are the z components of the Poynting vector associated exclusively with the transmitted, reflected, and incident waves, respectively. Although the power flows of the incident and reflected waves cannot be separated in an absorbing or gain medium, T and R are useful quantities if one deals with optical emitters and wants to compare the emitted powers in the presence and absence of the interface. Indeed, Eq. (7) can be written in terms of T_{12} as $S_2 = S_\infty e^{-2\alpha d} T_{12}$ where $S_\infty = 1/2 |E_0|^2 \text{Re}\{1/\eta_1^*\}$ is the Poynting vector in an infinite metamaterial in the absence of the interface. Hence, the plane-wave transmittance T_{12} has a transparent physical meaning also in an absorbing medium, showing the ratio of the transmitted Poynting vector to the infinite-medium Poynting vector at the same distance from the source. Note that in absorbing materials, one can obtain $T_{12} \neq T_{21}$, which means that *plane-wave transmission* through the interface

is not reciprocal. This interesting feature is usually omitted when considering absorbing materials, while the effect can be used for creation of more efficient optical absorbers and solar cells. Furthermore, T can be larger than 1, which shows that the emission can be more intense near an interface than in an infinite medium. From the point of view of improving the directionality of emission, the intensity of each plane-wave component yields the far-field intensity that is then the quantity of interest. For calculation of the total radiated power of a localized source, an entire angular spectrum must be considered. This is necessary when one is interested in, e.g., the lifetime modification of a fluorescent molecule by the Purcell effect.

III. EXAMPLES

In this section, we present simple metamaterial designs to showcase the effects described in Sec. II. In our first example we aim to demonstrate the enhancement of emission at the boundary of a *highly absorbing* metamaterial. The material is a metal-dielectric stack consisting of alternating layers of silver and glass, with thicknesses 30 nm and 100 nm, respectively [see Fig. 2(a)]. The period of the material is therefore $\Lambda_z = 130$ nm. This metamaterial behaves as a hyperbolic metamaterial at long wavelengths. We assume a refractive index $n = 1.5$ for glass and take the refractive index spectrum of Ag from [22]. Then, we use the wave parameter retrieval method of [18] to determine the refractive index and impedance for waves in the metamaterial propagating along the z axis. Figure 2(b) shows the spectrum of the refractive index that resembles the spectrum of a Drude metal with a plasma frequency at $\lambda_0 = 530$ nm. Figure 2(c) shows the wave impedance (normalized to that in vacuum) that is the core parameter for evaluating the emission enhancement. At $\lambda_0 \approx 530$ nm, both the real and imaginary parts of the impedance are large. Furthermore, Fig. 2(d) shows the spectra of ϵ and μ . The imaginary parts of these quantities are small, which implies relatively low absorption. We also note that $\text{Re}\{\mu\} > 1$, which is desirable because it increases the impedance.

We position an emitter exactly in the middle of one of the glass layers, as shown by the dashed line in the inset of Fig. 3(a), to minimize its quenching by the metal. Considering the metamaterial as a homogeneous medium with the retrieved n and η , we calculate the intensity of the plane-wave radiation at a distance of one unit cell from the source (the black dotted line). There are two cases to be considered: (1) the emitter is in an infinitely extended metamaterial as in the upper inset and (2) it is near the interface between the metamaterial and glass, as in the lower inset. The radiation spectra for these two cases are shown in Fig. 3(a) by the blue and red lines respectively. The spectra are normalized to the intensity of radiation that would take place in pure glass. Note that near $\lambda_0 = 530$ nm we have a large emission enhancement compared to the emission in glass in both cases.

It is remarkable, from the practical point of view, that the emission from inside the metamaterial into glass [the red curve in Fig. 3(a)] can exceed that in an infinite glass, even though the radiation is absorbed in the metamaterial and reflected by the interface. This is exactly the effect

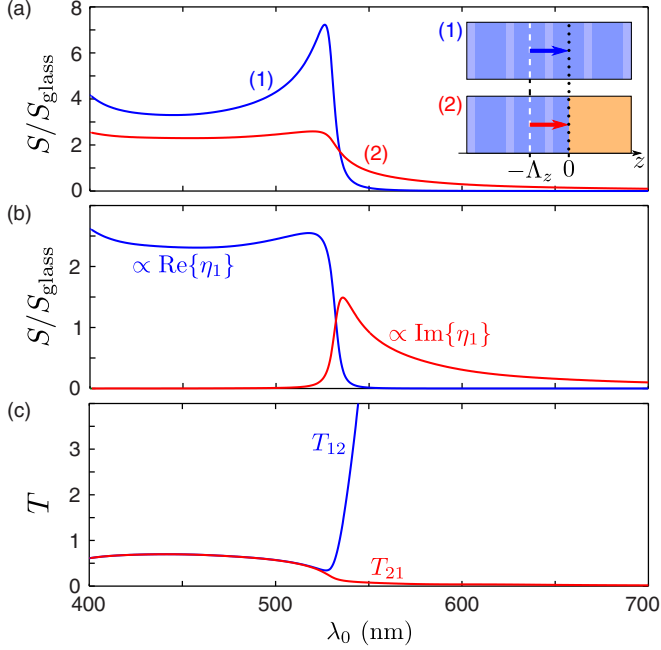


FIG. 3. Spectra of radiation from inside the metamaterial. In (a), the spectra show the intensity of radiation at $z = 0$ created by a plane-wave source at $z = -\Lambda_z$ inside the metal-dielectric stack metamaterial, normalized to the intensity of radiation in infinite glass. The dipole is either inside an infinite metamaterial [case (1), blue line] or at a distance Λ_z from the material interface with an ambient medium [case (2), red line]. The Poynting vector outside the material in case (2) is composed of two contributions, which are shown in (b). The terms proportional to $\text{Re}\{\eta\}$ and $\text{Im}\{\eta\}$ are shown with the blue and red curves, respectively. The effective plane-wave transmittances of the metamaterial-glass interface are shown in (c), T_{12} with a blue and T_{21} with a red line.

we wanted to demonstrate. At $\lambda_0 = 545$ nm, we have $S = S_{\text{glass}}$ for the transmitted field (see the red curve), as if the metamaterial was fully transparent glass. The contribution of the interference term in Eq. (5)—the one proportional to $\text{Im}\{\eta_1\}$ —to the radiation transmitted through the interface is shown in Fig. 3(b) by the red curve. The blue curve shows the contribution of the term proportional to $\text{Re}\{\eta_1\}$. It is obvious that the interference term makes a significant contribution to the radiation enhancement at $\lambda_0 > 530$ nm. The plane-wave transmittance T_{12} from the metamaterial to glass is shown by the blue curve in Fig. 3(c). At $\lambda_0 > 534$ nm, it increases above unity, implying that the transmitted power exceeds that flowing in an infinite metamaterial through the same plane (marked in the insets by the black dotted line). We also calculate the spectrum of the transmittance T_{21} from glass to the metamaterial and obtain the red curve in Fig. 3(c). For $\lambda_0 > 530$ nm, the difference between T_{12} and T_{21} is large and the wave transmission is clearly not reciprocal, as expected.

To confirm the above results and gain further insight into the radiation enhancement phenomenon we also study the wave energy flow in the structure microscopically, using direct numerical calculations on the basis of the COMSOL MULTIPHYSICS software. Fixing the wavelength at $\lambda_0 = 538.5$ nm, we calculated the distribution of the z component of the

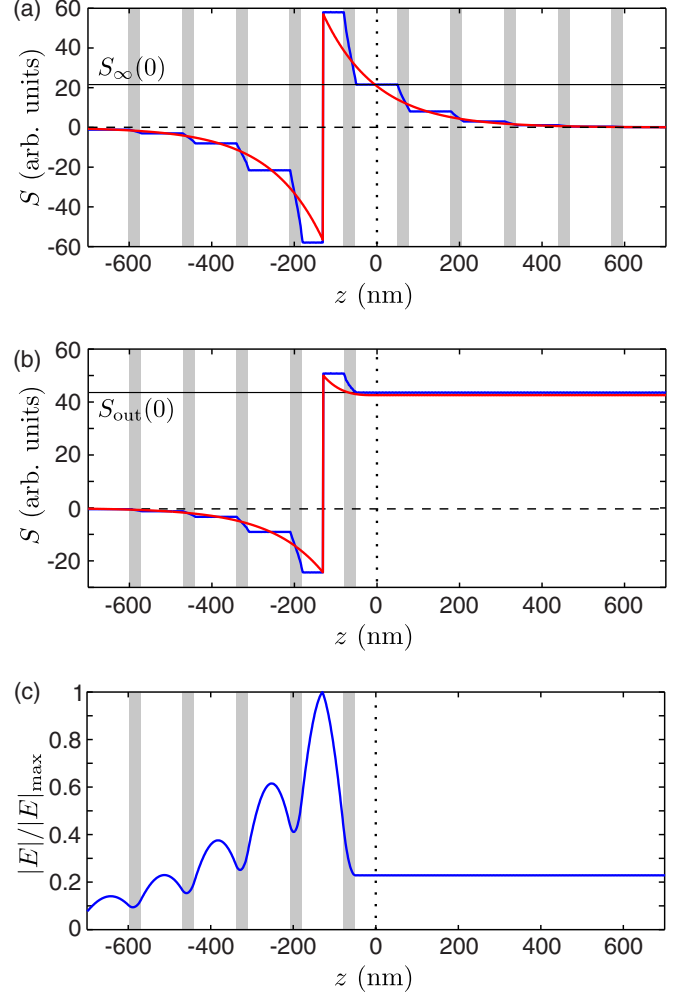


FIG. 4. Microscopic field distributions of light radiated from inside the metamaterial. The plane-wave radiation source is positioned at $z = -\Lambda_z$ (a) in an infinite metamaterial and (b) near the metamaterial-glass interface. The source emits at $\lambda_0 = 538.5$ nm. The gray areas show the position of the metal layers of the metamaterial. The blue curve shows the microscopic Poynting vector obtained by a full numerical simulation, while the red curve shows the Poynting vector as predicted by the wave parameter description. The values of the Poynting vectors at $z = 0$ are denoted by $S_{\infty}(0)$ and $S_{\text{out}}(0)$. (c) The microscopic electric-field amplitude corresponding to the case in (b).

Poynting vector along the z axis. The wave is generated by a planar source at $z = -\Lambda_z$ as before. Figures 4(a) and 4(b) show the results obtained for the infinite metamaterial and the metamaterial in contact with glass, respectively. The blue line shows the microscopic Poynting vector magnitude S and the red line the same quantity obtained for a homogenized metamaterial with the retrieved n and η (Figs. 2 and 3). The magnitude is negative where energy propagates to the left. It can be seen that in the middle of each glass layer of the structure, the red and blue lines coincide, confirming that our effective medium approach is correct. If the metamaterial is infinite, the wave propagating from the source to $z = 0$ attenuates in S by more than 50 %, which is in agreement with the retrieved $n = 0.08 + 0.33i$. However, when the source

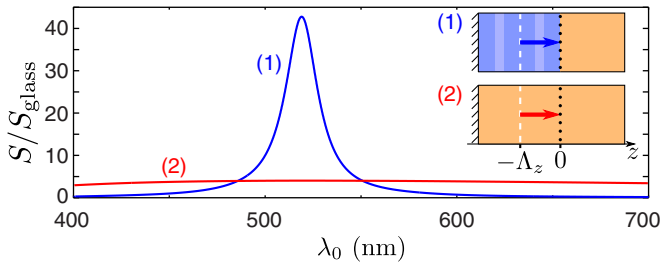


FIG. 5. Spectra of radiation from two systems shown in the insets: (1) source in the middle of a two-layer metamaterial slab on top of a silver mirror, and (2) the same source in glass, at a distance of ca. $\lambda/4$ from the mirror.

is near the boundary [see Fig. 4(b)], the attenuation upon propagation of the wave to $z = 0$ is lower, leading to a higher intensity of the wave released from the metamaterial to glass. The apparent transmission coefficient $T_{12} = S_{\text{out}}(0)/S_{\infty}(0)$ is equal to 2.1 [see the horizontal black lines in Figs. 4(a) and 4(b)], which is in agreement with Eq. (5).

The low attenuation and the resulting enhancement of the output radiation can also be understood by considering the distribution of the microscopic electric field in the structure. This distribution is shown in Fig. 4(c). The field is seen to be highly enhanced at the position of the source and within each glass layer by the wave interference effect. However, at the position of the metal plates, including the last one, the field has local minima, which leads to low attenuation, since the magnetic field does not contribute to absorption. This gives a microscopic explanation of the high output intensity correlating with the large negative value of $\text{Im}\{\eta_1\}$ and the prevailing electric absorption in the material. It is clearly different from the emission enhancement ordinarily obtained in hyperbolic metamaterials. In them the density of states is increased, while the interference effect in our material enhances the coupling of radiation to each existing mode. We consider the given example particularly interesting, because it can easily be realized in practice and tested also experimentally.

In the considered example, light emitted in the negative z direction (away from the glass-metamaterial interface) is lost, since it is not coupled out of the material. A practical way of eliminating this drawback is to reflect the radiation back to the interface with a mirror, which will enhance the *useful* radiation

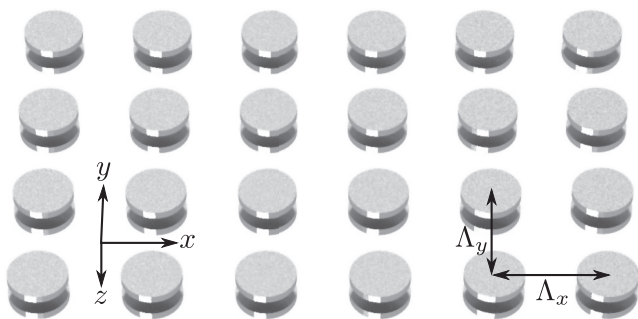


FIG. 6. A three-dimensional view of one layer of a disk-dimer metamaterial; the lattice is extended also in the z direction (not shown).

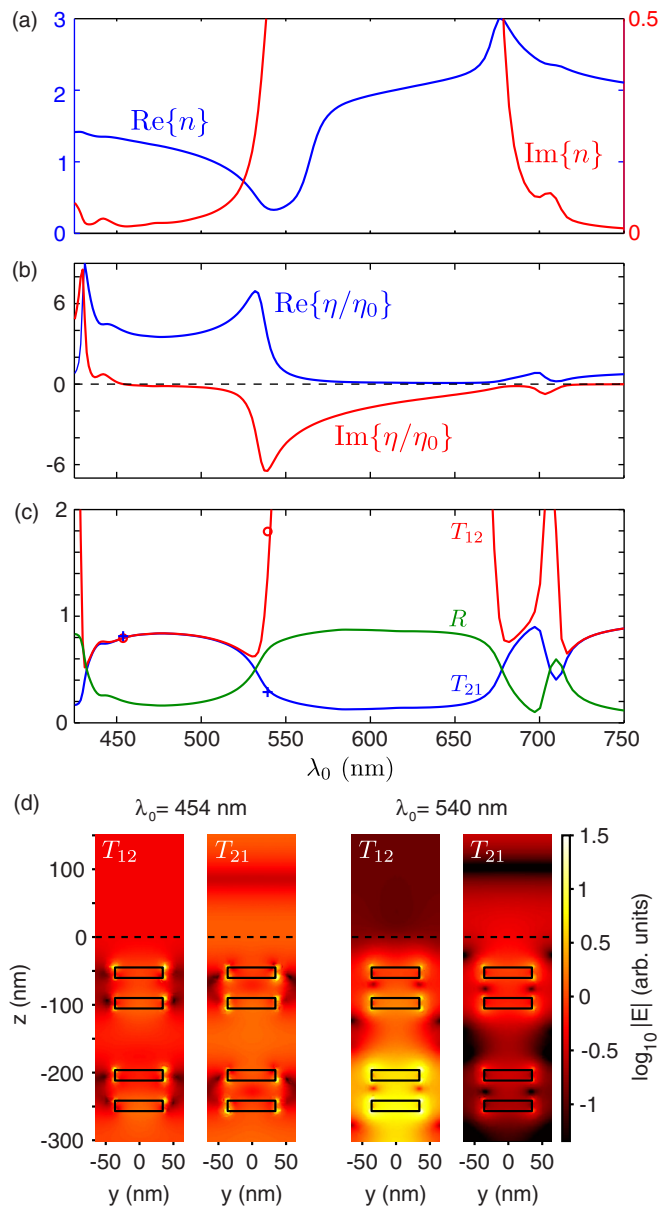


FIG. 7. Spectra of (a) refractive index and (b) impedance of the disk-dimer metamaterial for waves propagating along the z axis. In each plot, the blue line shows the real and the red line the imaginary part of the quantity. The spectra of the plane-wave transmittances T_{12} and T_{21} and reflectance R of the metamaterial-glass interface are shown in (c) with red, blue, and green curves, respectively. Full numerical simulation results are shown at two chosen wavelengths for both T_{12} (red circles) and T_{21} (blue crosses). The pictures of (d) are the distributions of electric-field amplitude in logarithmic scale at the chosen wavelengths and propagation directions.

into glass. In this case, one should use only a couple of the material's unit cells that, in addition, can be optimized for better enhancement. The inset (1) of Fig. 5 illustrates the setup. The material is otherwise the same as in Fig. 2 but the period is changed to $\Lambda = 150$ nm, to bring the emission enhancement maximum closer to the wavelength $\lambda_0 = 530$ nm considered previously. The source is placed between the two unit cells of the material. The mirror (tilted hatching) is made of silver.

In order to assess the effect of the metamaterial, we compare the emission enhancement in this case with a case of the same emitter placed in glass at an optimal distance (approximately $\lambda/4$) from the same mirror [see inset (2) of Fig. 5]. Figure 5 plots the spectrum of the output radiation in these two cases, relative to that in infinite glass. For the mirror-metamaterial system, in case (1), we achieve an emission enhancement factor of 43, while without the metamaterial, in case (2), the maximum enhancement factor is only 4. Therefore, combining the metamaterial with a mirror leads to a dramatic increase of the enhancement. Here one must note that in case (1) anything more than two unit cells of the metamaterial is unnecessary, as this will only add more absorption loss upon propagation of light toward the mirror and back.

Next we want to demonstrate an unusual absorbing metamaterial, in which the Poynting vectors of incident and reflected waves *are separable* as in a transparent material. For this, $\text{Im}\{\eta_1\}$ must be equal to 0, and therefore, the electric and magnetic fields must have equal contributions to the absorption. This property is interesting not only from the theoretical point of view, but also in view of applications to solar cells and perfect absorbers matched in impedance to air or glass and absorbing all the incident radiation.

We achieved the condition of $\text{Im}\{\eta_1\} = 0$ in an absorbing metamaterial illustrated in Fig. 6. The material consists of periodically distributed metamolecules in the form of paired silver disks in glass. The disks have a diameter of 70 nm and a thickness of 15 nm, and in each pair they are separated by a 30-nm surface-to-surface gap. These dimers form a tetragonal lattice with the periods $\Lambda_x = \Lambda_y = 130$ nm and $\Lambda_z = 150$ nm. We determine the wave parameters for this material using the same approach as in the previous example. Figure 7(a) shows the refractive index spectrum for a wave propagating along the z axis. The spectrum exhibits two resonances due to dipole and quadrupole excitations in the metamolecules [15,23,24]. Figure 7(b) shows the impedance spectrum. At $\lambda_0 = 454$ nm, there is a point of $\text{Im}\{\eta\} = 0$. At this wavelength, the incident and reflected waves should not exchange their energy via the interference phenomenon and the Poynting vector should not be spatially modulated. In this case, the transmittances T_{12} and T_{21} must be equal and such that $T_{12} + R_{12} = 1$. The spectra of the transmittances and the reflectance are presented in Fig. 7(c). One can see that at $\lambda_0 = 454$ nm, we indeed obtain $T_{12} = T_{21} = 0.8$ and $R_{12} = 0.2$ as for a fully transparent metamaterial. We have verified this condition by calculating T_{12} and T_{21} directly with COMSOL. The obtained values are shown together with the transmittance spectra with a red circle and a blue cross, which nearly perfectly overlap. The interference-cancellation regime is in fact approximately satisfied in a wide spectral range from 430 to 520 nm, as well as for $\lambda_0 > 720$ nm. In other regions, the magnitude

of $\text{Im}\{\eta\}$ is large, the Poynting vector is strongly modulated and T_{12} significantly exceeds T_{21} . We calculated the values of T_{12} and T_{21} directly numerically also for $\lambda_0 = 540$ nm, and again matched the wave parameter prediction nearly perfectly [see Fig. 7(c)]. The electric-field amplitude distributions at the chosen wavelengths and transmission directions are shown in Fig. 7(d). The horizontal dashed line marks the metamaterial-glass interface.

IV. CONCLUSIONS

We have introduced a theory that describes power flow in interfering optical waves inside an absorbing or amplifying nanomaterial with arbitrary refractive index and wave impedance. In particular, we have shown that the spatial modulation of absorption due to wave interference can make a layer of the material close to an interface effectively transparent, allowing light to escape from the material with negligible absorption and reflection losses. Furthermore, applying the theory to the light-emission phenomenon, we found that certain materials, despite being highly absorptive, can considerably enhance the output intensity of the emission when the emitter is situated inside the material. This type of enhancement is explained by strengthened coupling of the emitter to the existing plane-wave modes.

We considered two examples of optical nanomaterials. The first one was a metal-dielectric stack metamaterial exhibiting interference-induced transparency and far-field fluorescence enhancement. We also presented an application-oriented example by combining this material with a metal mirror, which produces an impressive radiation enhancement. The second example was a nanodimer metamaterial with a designed real-valued wave impedance, which eliminated the spatial modulation of absorption by interference. The electric- and magnetic-field components in this material make equal contributions to absorption, which makes the powers of the interfering waves separable as in a transparent material.

The discovered effects of the interference-induced transparency and enhancement of optical emission by a nanomaterial structure can be used to make nano- or microstructured optical sources, such as light-emitting diodes, more efficient. Our results challenge the notion that absorptive media are always detrimental to optical emission, inviting the design of new types of plasmonic metamaterials for fluorescence enhancement and other nano-optical applications. Since the approach is applicable also to materials with optical gain, it can find use also in lasers and laser amplifiers.

ACKNOWLEDGMENT

M.N. acknowledges financial support from the Finnish Cultural Foundation.

-
- [1] P. Anger, P. Bharadwaj, and L. Novotny, *Phys. Rev. Lett.* **96**, 113002 (2006).
 - [2] A. Poddubny, I. Iorsh, P. Belov, and Y. Kivshar, *Nat. Photon.* **7**, 948 (2013).
 - [3] M. A. Noginov, H. Li, Y. A. Barnakov, D. Dryden, G. Nataraj, G. Zhu, C. E. Bonner, M. Mayy, Z. Jacob, and E. E. Narimanov, *Opt. Lett.* **35**, 1863 (2010).
 - [4] D. Lu, J. J. Kan, E. E. Fullerton, and Z. Liu, *Nat. Nanotechnol.* **9**, 48 (2014).
 - [5] T. Galfsky, H. N. S. Krishnamoorthy, W. Newman, E. E. Narimanov, Z. Jacob, and V. M. Menon, *Optica* **2**, 62 (2015).
 - [6] L. Ferrari, D. Lu, D. Lepage, and Z. Liu, *Opt. Express* **22**, 4301 (2014).
 - [7] R. J. Potton, *Rep. Prog. Phys.* **67**, 717 (2004).

- [8] G. P. Ortiz and W. L. Mochán, *J. Opt. Soc. Am. A* **22**, 2827 (2005).
- [9] S.-C. Lee, *J. Opt. Soc. Am. A* **30**, 565 (2013).
- [10] M. A. Kats, R. Blanchard, P. Genevet, and F. Capasso, *Nat. Mater.* **12**, 20 (2012).
- [11] O. Deparis, *Opt. Lett.* **36**, 3960 (2011).
- [12] Y.-J. Jen, M.-J. Lin, H.-M. Wu, H.-S. Liao, and J.-W. Dai, *Opt. Express* **21**, 10259 (2013).
- [13] C. M. Soukoulis and M. Wegener, *Nat. Photon.* **5**, 523 (2011).
- [14] Z. Wang, F. Cheng, T. Winsor, and Y. Liu, *Nanotechnology* **27**, 412001 (2016).
- [15] P. Grahn, A. Shevchenko, and M. Kaivola, *Opt. Express* **21**, 23471 (2013).
- [16] A. Andryieuski, S. Ha, A. A. Sukhorukov, Y. S. Kivshar, and A. V. Lavrinenko, *Phys. Rev. B* **86**, 035127 (2012).
- [17] C. Menzel, C. Rockstuhl, T. Paul, F. Lederer, and T. Pertsch, *Phys. Rev. B* **77**, 195328 (2008).
- [18] A. Shevchenko, M. Nyman, V. Kivijärvi, and M. Kaivola, *Opt. Express* **25**, 8550 (2017).
- [19] Z.-L. Hou, M. Zhang, L.-B. Kong, H.-M. Fang, Z.-J. Li, H.-F. Zhou, H.-B. Jin, and M.-S. Cao, *Appl. Phys. Lett.* **103**, 162905 (2013).
- [20] J. D. Jackson, *Classical Electrodynamics* (Wiley, New York, 1975).
- [21] M. Nyman, V. Kivijärvi, A. Shevchenko, and M. Kaivola, *Phys. Rev. A* **95**, 043802 (2017).
- [22] P. B. Johnson and R. W. Christy, *Phys. Rev. B* **6**, 4370 (1972).
- [23] P. Grahn, A. Shevchenko, and M. Kaivola, *Phys. Rev. B* **86**, 035419 (2012).
- [24] A. Shevchenko, V. Kivijärvi, P. Grahn, M. Kaivola, and K. Lindfors, *Phys. Rev. Appl.* **4**, 024019 (2015).